Advanced Synthesis & Catalysis

Title: Copper(II)-Schiff Base Complex-Functionalized Polyacrylonitrile Fiber as a Green Efficient Heterogeneous Catalyst for One-Pot Multicomponent Syntheses of 1,2,3-Triazoles and Propargylamines

Authors: Pengyu Li, Yuanyuan Liu, Lu Wang, Jian Xiao, and Minli Tao

To be cited as: *Adv. Synth. Catal.* 10.1002/adsc.201701475

Link to VoR: http://dx.doi.org/10.1002/adsc.201701475

DOI: 10.1002/adsc.201

Copper(II)-Schiff Base Complex-Functionalized Polyacrylonitrile Fiber as a Green Efficient Heterogeneous Catalyst for One-Pot Multicomponent Syntheses of 1,2,3-Triazoles and Propargylamines

Pengyu Li,[a] Yuanyuan Liu,[a] Lu Wang,[a] Jian Xiao[a] and Minli Tao[a]*

[a] Department of Chemistry, School of Science Tianjin University
Collaborative Innovation Center of Chemical Science and Engineering.
Tianjin 300072, P. R. China.
E-mail: mltao@tju.edu.cn

Received:

Supporting information for this article is available on the WWW under http://dx.doi.org/10.1002/adsc.201######.

Abstract. A series of copper(II)-Schiff bases-functionalized polyacrylonitrile fiber catalysts were successfully prepared using copper acetate as copper source and characterized by elemental analysis, fourier-transfer infrared spectroscopy, ultraviolet-visible spectroscopy, X-ray photoelectron spectroscopy and inductively coupled plasma analysis. Excellent physical strength and thermal stability of the fiber catalysts were demonstrated by scanning electron microscopy, X-ray diffraction, thermogravimetric/ differential scanning calorimetry analysis and mechanical strength measurements. Furthermore, these catalysts were successfully applied to two one-pot multicomponent copper-catalyzed azide-alkyne cycloaddition (CuAAC) reaction and aldehyde, alkyne, amine (A3) coupling reaction in which the influences of different substituent groups on the catalytic activities of fiber catalysts were investigated in detail. Among them, the bis[*N*-ethyl-3,5-di-tert-butyl-salicylideneiminato]copper(II)-functionalized polyacrylonitrile fiber ($\mathrm{PAN_{S2}F}$-Cu) as a green, efficient catalyst exhibited the best catalytic activity for its high hydrophobic micro-environment can aggregate the reactants to the catalytic sites and accelerate the reaction. In addition, the $\mathrm{PAN_{S2}F}$-Cu has performed well in scaled-up experiment and shown excellent recyclability (at least ten times), and these enable it to have great potential for further applications.

Keywords: Polyacrylonitrile fiber; Schiff base; Copper catalyst; Triazoles; Propargylamines

Introduction

In current chemistry, natural products and other complicated organic compounds were synthesized by multistep synthetic strategies according to their complexity.[1] In such total synthesis procedures, disadvantages of low yields, tedious operation, high cost, environmental pollution, etc. restrict their large-scale applications in synthetic chemistry. Multicomponent reactions (MCRs), generally the one-pot reactions employing more than two starting materials, are reactions where most of the atoms of the starting materials are incorporated in the final products.[2] They are the most useful synthetic routes to generate great structural and skeletal complexes with advantages of simplicity, synthetic efficiency and atom-economy over conventional chemical syntheses.[3] For the advantages above, many MCRs such as Biginelli reaction,[4] Cu-catalyzed azide-alkyne cycloaddition (CuAAC) reaction,[5] Mannich reaction,[6] carbometallation-Michael reaction[7] and A3 coupling reaction,[8] have been applied in organic syntheses. Among them, Click chemistry (often synonymous with 1,3-dipolar cycloaddition to give triazoles) was introduced by Sharpless in 2001,[9] which is a set of powerful, highly reliable, selective and atom-efficient reaction in organic synthesis.[10] The products 1,2,3-triazoles have extensive applications in pharmaceutical,[11] chemical sensors,[12] biodegradable polymers[13] and so on. And A3 coupling reaction is a significant method to synthesis the propargylamines, which is an important skeleton structure of valuable intermediates[14] and biologically active compounds,[15] etc. Therefore, much attention has been paid to the MCRs of CuAAC and A3 coupling reactions.

In most cases, only catalyzed by appropriate catalysts can organic reactions take place smoothly with satisfactory yields.[16] Numerous homogeneous and heterogeneous catalysts have been designed and applied in various simple organic reactions or MCRs. However, homogeneous catalysis has the intrinsic disadvantage of complicated separation, which will cause resource consumption, environmental pollution and hinder its further application in industrial circle.

Compared to homogenous catalysts, heterogeneous ones have much advantages of facile separation and reusability of the catalysts and simple isolation of the product, which is a green strategy for sustainable chemistry. Immobilizing catalysts on solid supports is a common method to synthesize heterogeneous catalysts. Various organic materials like polymer,[5] cellulose,[17] chitosan,[18] starch,[19] resin,[20] and inorganic materials like SBA,[21] silica,[22] metallic oxide,[23] graphene,[24] activated carbon,[25] have been used as supports for heterogeneous catalysts. Due to the unique micro-environment, polymer supported catalysts often display superior catalytic activity, high regioselectivity and many other special performances.[26]

Polyacrylonitrile fiber (PANF), an industrial product of low cost, high strength, light density and mildew resistant, has been widely used in industry and our daily life. Because it has abundant cyano groups which can be easily transformed into carboxyl, aminocarbonyl and other functional groups.[27] More distinctively, the modification will reach hundred layers deep inside the fiber surface, which constructs a special soft micro-environment in favor of the accumulation of reactants and there by promoting the reaction.[26] Various PANF materials have been developed and applied to remove heavy metal ions[28] and organic compounds[29] from waste water or air, to prepare phase change material,[30] pH sensitive material,[31] antimicrobial material,[32] heterogeneous catalyst,[33] and so on. In our previous work, PANF not only has been modified to synthesize heavy metal ions adsorbent or sensory material[34] and acid-base sensory material,[27] but also been prepared into heterogeneous base catalyst,[35] acid catalyst,[36] phase transfer catalyst,[35b, 37] bifunctional catalyst,[38] metal catalyst[39] and chiral catalyst,[40] which indicate that the PANF is an ideal multipurpose support for heterogeneous catalyst.

Due to the economic and environmental friendly properties, copper catalyst has attracted the widespread attention of chemists. Numerous copper catalysts have been developed to efficiently catalyze various organic reactions.[41] In the present study, combining the advantages of copper catalyst and PANF, and several Cu(II)-Schiff base complexes-functionalized PANFs have been prepared and applied to MCRs of CuAAC and A3 coupling reactions as efficient green reusable heterogeneous catalysts.

Results and Discussion

Synthesis of the fiber catalysts

The fiber catalysts PAN$_{E}$F-Cu and PAN$_{S1-5}$F-Cu were prepared as shown in scheme 1. In the first step, PANF was refluxed with ethylenediamine aqueous to get the PAN$_{E}$F (modified degree = 2.4 mmol/g) which was treated with different aldehydes to give the Schiff base modified PAN$_{S1-5}$F. Finally, the formed PAN$_{S1-5}$F were coordinated with $Cu(OAc)_2$ to obtain the green fiber catalysts PAN$_{S1-5}$F-Cu. On the other hand, the PAN$_{E}$F can coordinate with $Cu(OAc)_2$ directly to synthesize the PAN$_{E}$F-Cu as another fiber catalyst. The extents of functionalization of the fibers were determined by weight gain and ICP analysis which were summarized in Table 1.

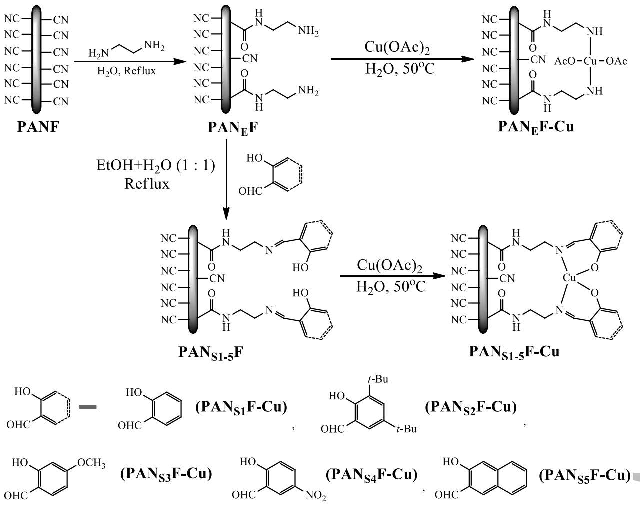

Scheme 1. Preparation of the fiber catalysts.

The Schiff base contents are approximately double that of the copper (Table 1, entries 1-3), which indicates that one copper ion chelates with two Schiff base units (Scheme 1). While for PAN$_{S4}$F-Cu and PAN$_{S5}$F-Cu, rarely coppers are anchored on the fiber. This result has been proved by the elemental analysis, FTIR and UV-vis spectra. That may be explained by the low coordination abilities of the Schiff bases due to the strong electron-withdrawing group or large conjugate aromatic ring (Table 1, entries 5 and 6).

Elemental analysis (EA)

The EA data of PANF and modified fibers are displayed in Table 2 and Table S1. With the introduction of amide oxygen atom and the aminoethyl group, the PAN$_{E}$F has lower carbon and nitrogen contents (62.87% and 23.09%, respectively) and higher hydrogen content (6.263%) (Table 2, entry 2). Because the Schiff base moieties in PAN$_{S2}$F have

Table 1. The modified degree of fiber catalysts.

Entry	Fiber	C_S (mmol/g)$^{a)}$	C_{Cu} (mmol/g)$^{b)}$
1	PAN$_{S1}$F-Cu	2.0	1.25
2	PAN$_{S2}$F-Cu	1.97	1.11
3	PAN$_{S3}$F-Cu	1.80	1.13
4	PAN$_{S4}$F-Cu	2.27	0.02
5	PAN$_{S5}$F-Cu	2.18	0.05
6	PAN$_{E}$F-Cu	----	0.55

$^{a)}$ C_S: Schiff base contents of different fibers, which determined by weight gain. Weight gain = [(*W2*-*W1*)/*W1*] ×100%, where *W1* and *W2* are the weights of unmodified and modified fibers. $^{b)}$ C_{Cu}: Cu contents of different fibers, which determined by ICP.

Table 2. EA data of different fibers.

Entry	Fiber	C (%)	H (%)	N (%)	S (%)
1	PANF	70.75	5.94	26.12	0.09
2	PAN$_E$F	62.87	6.26	23.09	0.01
3	PAN$_{S2}$F	66.94	7.10	16.29	0.01
4	PAN$_{S2}$F-Cu	60.76	6.48	15.43	0.01
5	PAN$_{S2}$F-1[a)]	60.95	6.51	15.81	0.01
6	PAN$_{S2}$F-10[b)]	61.81	6.63	16.55	0.01

[a)] The PAN$_{S2}$F-Cu was used once in CuAAC reaction. [b)] The PAN$_{S2}$F-Cu was used ten times in CuAAC reaction.

higher carbon and hydrogen contents and lower nitrogen content, the carbon and hydrogen contents rise to 66.94% and 7.10% respectively, and the nitrogen content of PAN$_{S2}$F declined to 16.29% (Table 2, entry 3). When Schiff base moieties in PAN$_{S2}$F coordinate with copper ions, all the carbon, hydrogen and nitrogen contents of the fiber catalyst PAN$_{S2}$F-Cu declined (Table 2, entry 4). After the fiber catalyst was used once in CuAAC reaction, the PAN$_{S2}$F-Cu-1 remained almost the same EA data with that of the fresh fiber catalyst (Table 2, entry 5). While, when the fiber catalyst is reused ten times, the carbon and nitrogen contents of PAN$_{S2}$F-Cu-10 respectively increased to 61.81% and 16.55%, which may be attributed to the absorption of organic compounds during the reaction process (Table 2, entry 6). The EA data of fiber catalysts PAN$_{S1}$F-Cu and PAN$_{S3}$F-Cu are listed in table S1 which are similar with that of PAN$_{S2}$F-Cu. However, because of the poor chelate abilities of PAN$_{S4}$F and PAN$_{S5}$F, the EA data of PAN$_{S4}$F-Cu and PAN$_{S5}$F-Cu are almost no changes compared to that of PAN$_{S4}$F and PAN$_{S4}$F, respectively (Table S1, entries 5-8).

Fourier-transfer infrared spectroscopy (FTIR)

Samples of PANF, PAN$_E$F, PAN$_{S2}$F, PAN$_{S2}$F-Cu, PAN$_{S2}$F-Cu-1 and PAN$_{S2}$F-Cu-10 were pulverized by cutting and then prepared into KBr pellets, and their FTIR spectra are shown in Figure 1. For PANF, the distinctive absorption band at 2244 cm^{-1} is attributed to C≡N stretching vibrations. Due to the existence of methyl acrylate units in PANF, there is C=O stretching vibration peak at 1737 cm^{-1}. Moreover, the strong absorption band at 1455 cm^{-1} is assigned to the C-H bending vibrations (Figure 1a). After being modified by ethylenediamine (Figure 1b), methoxycarbonyl and cyano groups react with -NH$_2$, and the bands at 1733 cm^{-1} and 2245 cm^{-1} are weakened apparently and two strong bands appeared at 1654 cm^{-1} and 1561 cm^{-1} which are attributed to the amide I and II bands, respectively. Besides, the new broad band at 3650-3150 cm^{-1} is stretching vibration peak of N-H in -NH$_2$. In the spectrum of PAN$_{S2}$F-EA (Figure 1c), the peak at 1644 cm^{-1} is enhanced which is caused by the formation of C=N bond. The spectrum of PAN$_{S2}$F-Cu (Figure 1d) shows a red shift to 1622 cm^{-1} due to the coordination of the C=N band with copper ions.[24, 42] The FTIR spectra of PAN$_{S1}$F-Cu (Figure S2d) and PAN$_{S3}$F-Cu (Figure S2f) have similar red-shift phenomena. Therefore, the Cu-Schiff base complexes are proved to be grafted onto the fiber successfully. However, the spectrum of PAN$_{S4}$F-Cu and PAN$_{S5}$F-Cu are nearly the same with PAN$_{S4}$F and PAN$_{S5}$F, which indicate the copper ions and Schiff base complexes are almost no coordinating (Figure S2g-j). After the PAN$_{S2}$F-Cu was reused one or ten times, the FTIR spectra of PAN$_{S2}$F-Cu-1 and PAN$_{S2}$F-Cu-10 only have minor changes, which suggests the excellent recoverability of the fiber catalyst (Figure 1e and f).

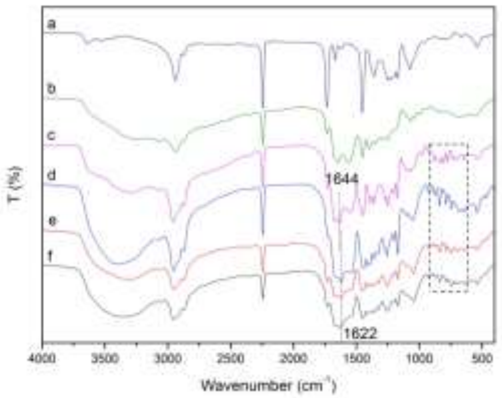

Figure 1. FTIR spectra of (a) PANF, (b) PAN$_E$F, (c) PAN$_{S2}$F, (d) PAN$_{S2}$F-Cu, (e) PAN$_{S2}$F-Cu-1, (f) PAN$_{S2}$F-Cu-10.

Solid UV-Vis spectroscopy

The fiber catalysts are also investigated by solid UV-Vis technique and the results are shown in Figure 2. Compared with PANF and PAN$_E$F, the UV-Vis spectrum of PAN$_{S2}$F shows a distinct new peak around 360 nm which is due to the $\pi\rightarrow\pi^*$ and $n\rightarrow\pi^*$ transitions of the Schiff base moiety.[42] New bands

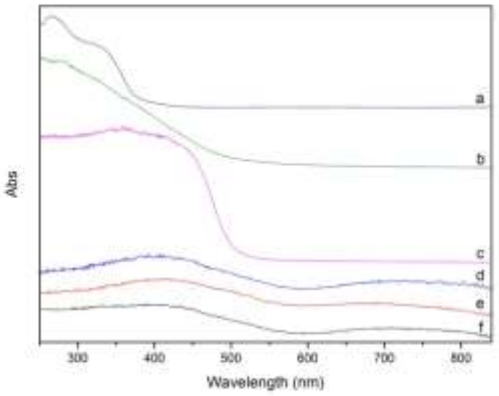

Figure 2. UV-vis spectra of (a) PANF, (b) PAN$_E$F, (c) PAN$_{S2}$F, (d) PAN$_{S2}$F-Cu, (e) PAN$_{S2}$F-Cu-1, (f) PAN$_{S2}$F-Cu-10.

around 420 nm and 730 nm appeared in spectrum of PAN$_{S2}$F-Cu are attributed to the ligand to metal transfer (LMCT) and *d*→*d* transition band of the Cu(II), respectively.[43] The UV-Vis spectra of PAN$_E$F-Cu (Figure S3a), PAN$_{S1}$F-Cu (Figure S3c) and PAN$_{S3}$F-Cu (Figure S3e) are similar to PAN$_{S2}$F-Cu which indicate the successful anchoring of Cu(II) Schiff base complexes on PANF. As well as FTIR spectra, the UV-Vis spectra of PAN$_{S4}$F-Cu and PAN$_{S5}$F-Cu (Figure S3g and i) don't show similar peak as PAN$_{S2}$F-Cu. After reused one or ten times in CuAAC reaction, the PAN$_{S2}$F-Cu shows excellent stability because the spectra of PAN$_{S2}$F-Cu-1 (Figure 2e) and PAN$_{S2}$F-Cu-10 (Figure 2f) are basically consistent.

Scanning electron microscopy (SEM)

The SEM images of PANF, PAN$_E$F, PAN$_{S2}$F, PAN$_{S2}$F-Cu, PAN$_{S2}$F-Cu-1 and PAN$_{S2}$F-Cu-10 are shown in Figure 3. The diameter of PANF is around 25 μm and the surface is smooth (Figure 3a). After modified succeedingly by ethylenediamine, aldehyde and Cu(OAc)$_2$, the surface of the fiber becomes slightly rough, and the diameter increases remarkably (Figure 3b, c and d), which indicates the successful grafting of Schiff base-Cu. When the fiber catalyst was used once, very few changes occur on the fiber catalyst surface (Figure 3e). While, after being reused ten times, the surface of the PAN$_{S2}$F-Cu-10 becomes more roughly and the diameter becomes more slender (Figure 3f). In the end, the basic structure of fiber catalyst is retained with considerable mechanical strength which will be confirmed by further research (Table 3), for example, the PAN$_{S2}$F-Cu-10 still keeps 72% mechanical strength as the original PANF (Table 3, entry 6).

X-ray photoelectron spectroscopy (XPS)

The XPS spectra of PAN$_{S2}$F-Cu are shown in Figure 4. The surface content of copper calculated by XPS is 0.78 mmol/g, which is less than the total copper content of 1.11 mmol/g tested by ICP. The result illustrates that the fiber catalyst is not modified on shallow surface but a goes deep to multilayers which further contribute to the formation of catalytic micro-environments on the fiber catalyst. High intensity peaks at 933.4 eV, 953.1 eV and satellite peaks around 942.8 eV could be assigned to the characteristic binding energies of Cu(II) (Figure 4b) which shows the successful immobilization of Cu(II).[44]

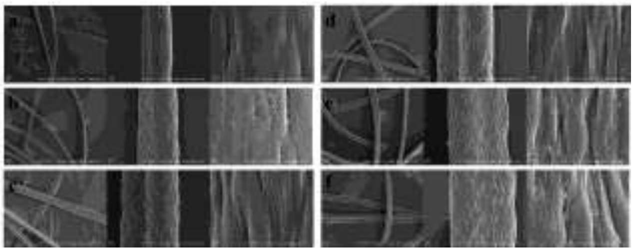

Figure 3. SEM images of (a) PANF, (b) PAN$_E$F, (c) PAN$_{S2}$F, (d) PAN$_{S2}$F-Cu, (e) PAN$_{S2}$F-Cu-1, (f) PAN$_{S2}$F-Cu-10.

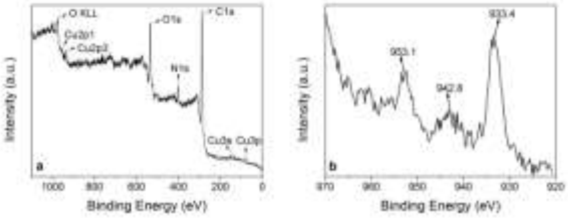

Figure 4. XPS spectra of PAN$_{S2}$F-Cu: (a) survey spectrum, (b) Cu2p spectrum.

X-ray diffraction (XRD).

Different fibers were also studied by XRD, and the spectra of PANF, PAN$_E$F, PAN$_{S2}$F and PAN$_{S2}$F-Cu are given in Figure 5. For PANF, two peaks (2θ=17º, 30º) are shown in Figure 5a which correspond to strong diffraction of (100) face and weak diffraction of (110) face, respectively. The intense peak at 2θ=17º is due to the hexagonal lattice formed by the parallel close packing of the molecule rods.[45] The peak at 17º in Figure 5b is stronger than that of PANF because that some ethylenediamine molecules crosslink between the fiber skeletons to stabilize the structure of PANF. For spectra of PAN$_{S2}$F, PAN$_{S2}$F-Cu and PAN$_{S2}$F-Cu-10 (Figure 5c-e), the peaks at 17º are weaker than that of PANF and PAN$_E$F, which indicates that part of the crystalline phase of the fibers have been changed after being heated during the modification process.

Thermal Stability Analysis

TG/DSC curves of different fibers are presented in Figure 6. The maximum thermal decomposition

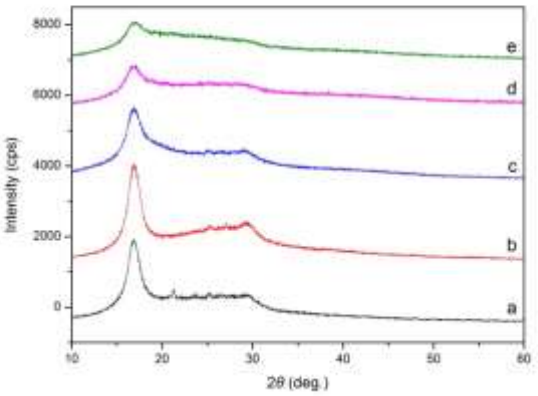

Figure 5. X-ray diffraction spectra of (a) PANF, (b) PAN$_E$F, (c) PAN$_{S2}$F, (d) PAN$_{S2}$F-Cu, (e) PAN$_{S2}$F-Cu-10.

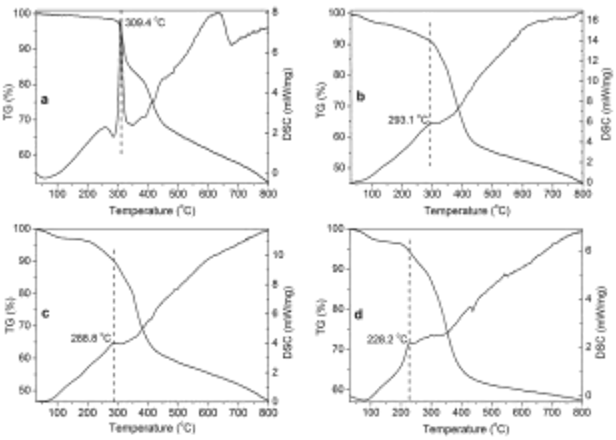

Figure 6. TG/DSC spectra of (a) PANF, (b) PAN$_E$F, (c) PAN$_{S2}$F, (d) PAN$_{S2}$F-Cu.

temperature (DSCmax) of the PANF is determined to be 309.4 (Figure 6a). After modified by ethylenediamine, the DSCmax of PAN$_E$F is slightly declined to 293.1 °C, which indicates very little damage happening on the fiber. In addition, the decreasing rate of the PAN$_E$F's TG curve is slower than that of PANF (Figure 6b) due to the crosslinking of ethylenediamine with PANF. The PAN$_{S2}$F exhibites a main transient of weight loss at 288.8 °C, which shows similar thermal stability with that of PAN$_E$F (Figure 6c). Although the DSCmax of PAN$_{S2}$F-Cu further declines to 228.2 °C (Figure 6d), it is enough for the application in CuAAC and A3 coupling reactions. Furthermore, when the fiber is heated to 800 °C, the PAN$_{S2}$F-Cu has a mass residue of 57.4%, which is 10.5% higher than that of the PAN$_{S2}$F (46.9%). The higher mass residue of PAN$_{S2}$F-Cu shoud be attributed to the immobilization of copper. The copper content by the mass residue is 1.64 mmol/g which higher than the copper content tested by ICP (1.11 mmol/g), which may be because part of copper ions are coordinate with Schiff base moieties as a ratio of 1:1 (Scheme S1) and systematic errors of different methods. In summary, all experiment results can prove the successful immobilization of copper on the fiber.

Mechanical strength

The breaking strength (BS) is an important application indicator for the fiber catalysts. Higher mechanical strength will make the fiber catalyst more suitable for the application as fixed bed material in industry. The testing results of breaking strength (BS) and retention of breaking strength (RBS) of different fibers are listed in Table 3. After grafting with the Schiff base, the breaking strength of PAN$_{S2}$F decreases to 9.1 cN with 83% RBS (Table 3, entry 2). The processes of anchoring copper ion have less impact on the mechanical strength of fiber catalysts, so PAN$_{S2}$F-Cu almost keep its break strength with 79% RBS (Table 3, entry 3). When the fiber catalyst was applied to the CuAAC reaction of benzyl chloride, phenyl acetylene and sodium azide once, the RBS of the PAN$_{S2}$F-Cu-1 is the same with that of PAN$_{S2}$F-Cu (Table 3, entries 4 and 5). After reused ten times, 72% RBS of PAN$_{S2}$F-Cu-10 is still reserved (Table 3, entry 6). That shows the PAN$_{S2}$F-Cu has good mechanical strength for further researches.

Table 3. The mechanical properties of different fibers.

Entry	Fiber	BS (cN)	RBS (%)
1	PANF	11.0	100
2	PAN$_{S2}$F	9.1	83
3	PAN$_{S2}$F-Cu	8.7	79
4	PAN$_{S2}$F-Cu-1	8.7	79
5	PAN$_{S2}$F-Cu-10	7.9	72

Catalytic activities

Initially, the Cu(II)-Schiff base-functionalized fibers

Table 4. Optimization of the CuAAC reaction conditions.$^{a)}$

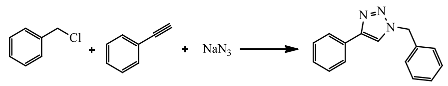

1a

Entry	Catalyst	Solvent	T (°C)	Time (h)	Yield (%)$^{b)}$/TON
1	----	H_2O	60	2	2/----
2	PANF	H_2O	60	2	2/----
3	$Cu(OAc)_2$	H_2O	60	2	41/20.5
4	S2-Cu$^{c)}$	H_2O	60	2	67/33.5
5	PAN$_{S1}$F-Cu	H_2O	60	2	51/25.5
6	PAN$_{S2}$F-Cu	H_2O	60	2	66/33.0
7	PAN$_{S3}$F-Cu	H_2O	60	2	32/16.0
8	PAN$_{S4}$F-Cu	H_2O	60	2	11/5.5
9	PAN$_{S5}$F-Cu	H_2O	60	2	13/6.5
10	PAN$_E$F-Cu	H_2O	60	2	51/25.5
11	PAN$_{S2}$F-Cu	H_2O	60	3	85/42.5
12	PAN$_{S2}$F-Cu	H_2O	60	3.5	97/48.5
13	PAN$_{S2}$F-Cu	H_2O	60	4	97/48.5
14	PAN$_{S2}$F-Cu	H_2O	80	3.5	97/48.5
15	PAN$_{S2}$F-Cu	H_2O	50	3.5	84/42.0
16$^{d)}$	PAN$_{S2}$F-Cu	H_2O	60	3.5	96/19.6
17$^{e)}$	PAN$_{S2}$F-Cu	H_2O	60	3.5	91/93.0
18$^{f)}$	PAN$_{S2}$F-Cu	H_2O	60	3.5	78/156
19$^{g)}$	PAN$_{S2}$F-Cu	H_2O	60	3.5	18/360
20$^{g)}$	PAN$_{S2}$F-Cu	H_2O	60	24	98/1960
21	PAN$_{S2}$F-Cu	CH_3OH	60	3.5	19/9.5
22	PAN$_{S2}$F-Cu	C_2H_5OH	60	3.5	4/2
23	PAN$_{S2}$F-Cu	CH_3CN	60	3.5	1/0.5
24	PAN$_{S2}$F-Cu	1,4-Dioxane	60	3.5	0/0
25	PAN$_{S2}$F-Cu	AcOEt	60	3.5	0/0

$^{a)}$ Reaction conditions: benzyl chloride (1 mmol), phenylacetylene (1 mmol), NaN_3 (1.2 mmol), *L*- sodium ascorbate (10 mol%), catalyst (2 mol%, calculate base on Cu) and solvent (5 mL). $^{b)}$ Yield by HPLC. $^{c)}$ The structure of S2-Cu was shown in supporting information. $^{d)}$ With 5 mol% catalyst. $^{e)}$ With 1 mol% catalyst. $^{f)}$ With 0.5 mol% catalyst. $^{g)}$ With 0.05 mol% catalyst.

were used to catalyze the CuAAC reaction and the results are listed in Table 4.When the reaction was carried out without catalyst or in the presence of PANF, only 2% yield was obtained (Table 4, entries 1 and 2). In the case of $Cu(OAc)_2$ or S2-Cu as catalysts, the yield were raised to 41% and 67%, respectively (Table 4, entries 3 and 4). With $PAN_{S1\text{-}3}F$-Cu as catalysts, yields of 32-66% were obtained (Table4, entries 5-7). And the $PAN_{S2}F$-Cu shows the same catalytic activity with S2-Cu (Table 4, entry 6). That may be because the special flexible micro-environment of the fiber catalyst can efficiently aggregate the reactants to the catalytic active center and accelerate the reaction. Especially, the hydrophobic micro-environment constructed by the Schiff base with two tertiary butyl groups will promote the reaction more efficiently.[46] The catalytic activity of $PAN_{S3}F$-Cu is lower than that of $PAN_{S1}F$-Cu and $PAN_{S2}F$-Cu (Table 4, entries 5-7) due to the electron donating effect of the $-OCH_3$ in $PAN_{S3}F$-Cu, which declines the reaction activity of alkyne-copper intermediate with iminium ion intermediate generated from aldehyde and secondary amine.[47] Because of the low contents of Cu, there has few valid catalytic active sites on $PAN_{S4}F$-Cu and $PAN_{S5}F$-Cu, only 11% and 13% yields were obtained (Table 4, entries 8 and 9). For $PAN_{E}F$-Cu, although a medium yield 51% was obtained, the fiber changed color from green to yellow after reaction, which indicates the Cu has dissociated from the fiber (Table 4, entry 10). When the reaction time was prolonged from 2 h to 3.5 h with $PAN_{S2}F$-Cu as catalyst, the yields increased from 66% to 97% (Table 4, entries 6, 11 and 12). Reducing the reaction temperature to 50ºC will cause yield fall down to 84% (Table 4, entry 15). However, there has no obvious yield improvement with longer reaction time or higher temperature (Table 4, entries 13 and 14). When increasing the catalyst amount to 5 mol%, a yield of 96% was obtained. If the catalyst amount was decreased to 1 mol%, 0.5 mol% and 0.05 mol%, the yields were declined to 91%, 78% and 18 % respectively (Table 4, entries 16-19). Nevertheless, the reaction can also be finished with catalyst amount of 0.05 mol% when the reaction time was prolonged to 24 h (Table 4, entry 20). And the highest TON of 1960 was attained with 0.05 mol% catalyst amount. Furthermore, the solvent effect on the CuAAC reaction had also been explored. The yields obviously decreased as lowering the solvent polarities (Table 4, entries 21-25). With solvent polarities lower than CH_3CN, the reaction even failed to take place (Table 4, entries 24 and 25). All in all, the optimal conditions with $PAN_{S2}F$-Cu as catalyst are 3.5 h at 60ºC in water.

Under the optimal conditions, we probed the scope of the reaction with different halohydrocarbons and

Table 5. The substrate scope CuAAC reaction catalyzed by $PAN_{S2}F$-Cu.[a)]

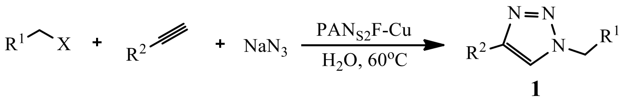

Entry	X	R^1	R^2	Time (h)	Yield (%)[b)]
1	Cl	C_6H_5	C_6H_5	3.5	**1a** 95
2	Br	C_6H_5	C_6H_5	2	**1a** 97
3	Cl	$4\text{-}MeC_6H_5$	C_6H_5	3.5	**1b** 94
4	Cl	$4\text{-}ClC_6H_5$	C_6H_5	3.5	**1c** 95
5	Cl	$4\text{-}CNC_6H_5$	C_6H_5	3.5	**1d** 95
6	Br	$4\text{-}CNC_6H_5$	C_6H_5	2	**1d** 98
7	Cl	$2\text{-}CNC_6H_5$	C_6H_5	3.5	**1e** 96
8	Cl	EtOOC	C_6H_5	5	**1f** 90
9	Br	EtOOC	C_6H_5	3	**1f** 92
10	Cl	3-CHO-2-OHC_6H_3	C_6H_5	3.5	**1g** 89
11	Br	$4\text{-}BrC_6H_5$	C_6H_5	2	**1h** 96
12	Br	$4\text{-}NO_2C_6H_5$	C_6H_5	2	**1i** 97
13	Br	$3\text{-}NO_2C_6H_5$	C_6H_5	2	**1j** 97
14	Br	C_6H_5CO	C_6H_5	3	**1k** 91
15	Br	$n\text{-}C_3H_7$	C_6H_5	5	**1l** 94
16	Br	C_6H_5	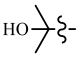 HO	5	**1m** 95
17	Br	$4\text{-}BrC_6H_5$	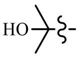 HO	4	**1n** 93
18	Br	$4\text{-}CNC_6H_5$	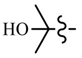 HO	5	**1o** 97
19	Br	C_6H_5	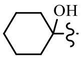 OH	5	**1p** 90
20	Br	$4\text{-}BrC_6H_5$	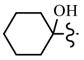 OH	4	**1q** 95
21	Br	$4\text{-}CNC_6H_5$	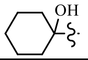 OH	5	**1r** 93

[a)] Reaction conditions: halohydrocarbon (1 mmol), alkynes (1 mmol), NaN_3 (1.2 mmol), *L*-sodium ascorbate (10 mol%), catalyst (2 mol%, calculate base on Cu) and solvent (5 mL). [b)] Isolate yield.

Table 6. $PAN_{S2}F$-Cu catalyzed synthesis of bis-and tris-triazoles.[a)]

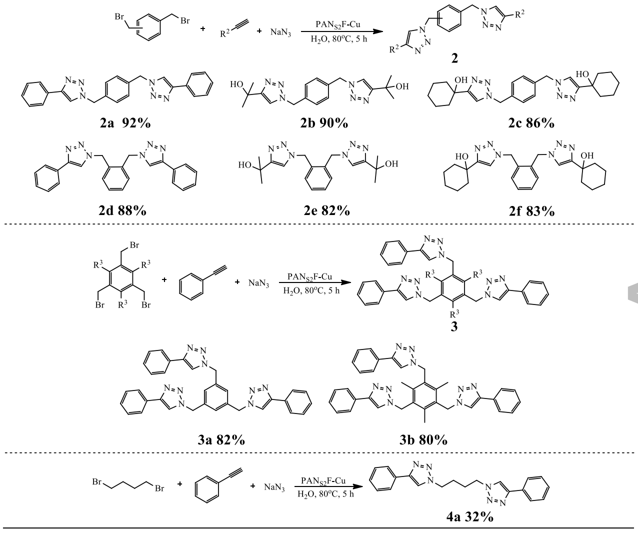

[a)] Reaction conditions: halohydrocarbon (1 mmol), alkynes (2 mmol), NaN_3 (2.5 mmol), *L*-sodium ascorbate (10 mol% based on alkynes), catalyst (2 mol%, calculate base on Cu) and solvent (5 mL). Isolate yield.

alkynes. As shown in Table 5, the activities of bromo-hydrocarbons are higher than that of chloro-ones (Table 5, entries 1-15). Excellent yields are obtained whether the substituents are electron-donating or electron-withdrawing groups on phenyl groups which coincied with literature results.[25] In addition, the scope of different alkynes can also obtain excellent yields of 93-97% (Table 5, entries 16-21).

Encouraged by the excellent results above, the activity of this catalytic system was further tested by catalyzing the synthesis of several bis- and tris-triazoles. In Table 6, 1,2-bisbromomethylbenzens and 1,4-bisbromomethylbenzene can both react smoothly with different alkynes catalyzed by fiber PAN$_{S2}$F-Cu to achieve 82-92% yields (Table 6, 6a-f). The activity of 1,2-bisbromomethylbenzene is lower than that of 1,4-bisbromomethylbenzene which may be caused by the larger steric hindrance of the former. Furthermore, the tris-triazoles were synthesized successfully with yields of 80-82% in 5 h at 80ºC (Table 6, 8a-b). However, only 32% yield was obtained for the 1,4-dibromobutane due to the low activity of the bromoalkane (Table 6, 9a).

To further widen the applicability of the present methodology, the catalytic activity of this catalytic system was also examined by the A3 coupling reaction which is an important reaction in organic synthesis.[8] In the first place, the A3 reaction was carried out in different solvents. From Table 7 we can see that, high polarity solvent is beneficial for the A3 reaction especially in CH_3CN (with a yield of 53% in 3 h). When the temperature was raised to 80ºC, the yield increased obviously to 68% in 3 h (Table 7, entry 9). Prolonging the reaction time from 3 h to 6 h, the yields improved from 53% to 95% gradually (Table 7, entries 9-12). The yield no longer increased when reaction time was prolonged to 7 h (Table 7, entry 13).

Universality of the fiber catalyst PAN$_{S2}$F-Cu in three-component coupling reaction was determined by different combinations of aldehydes, amines and alkynes and the results are shown in Table 8. Comparing different amines, pyrrolidine has higher yield than diethylamine and dibutylamine (Table 8, entries 1-3) since the iminium ion produced from alicyclic amine is more stable than that of dialkyl amine.[48] Because of the low activities of aromatic aldehydes caused by conjugate effect, the yields of aromatic aldehydes are lower than that of aliphatic aldehydes (Table 8, entries 4-13). Besides, aromatic aldehydes with electron-withdrawing groups have higher yields than that of aromatic aldehydes with electron-donating groups (Table 8, entries 7-13).

Possible mechanisms of the CuAAC reaction and A3 coupling reaction catalyzed by PAN$_{S2}$F-Cu were depicted in Scheme 2. Both of the two reactions have some parallel procedures. Initially, the Cu(II) on the fiber catalyst was reduced by sodium ascorbate to PAN$_{S2}$F-Cu(I) which can efficiently activate the C-H bond of alkyne to form the intermediate **A**. For A3 reaction, the intermediate **A** was then reacted with the iminium ion intermediate **B** generated from aldehyde and secondary amine to give the propargylamines. In terms of CuAAC reaction, the corresponding 1,2,3-triazoles were produced after the reaction of intermediate **A** with azides **C** generated from halohydrocarbons and NaN_3. After the above processes, the fiber catalyst was regenerated for further reaction.

Table 7. Optimization of the A3 coupling reaction conditions.[a)]

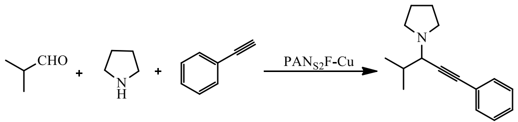

5d

Entry	Solvent	T (ºC)	Time (h)	Yield (%)[b)]
1	H_2O	60	3	27
2	CH_3OH	60	3	26
3	C_2H_5OH	60	3	37
4	CH_3CN	60	3	53
5	THF	60	3	16
6	EtOAc	60	3	2
7	Toluene	60	3	13
8	Cyclohexane	60	3	3
9	CH_3CN	80	3	68
10	CH_3CN	80	4	85
11	CH_3CN	80	5	92
12	CH_3CN	80	6	95
13	CH_3CN	80	7	95

[a)] Reaction conditions: isobutyraldehyde (1 mmol), pyrrolidine (1 mmol), phenylacetylene (1.2 mmol), *L*-sodium ascorbate (10 mol%), catalyst (2 mol%, calculate base on Cu) and solvent (5 mL). [b)] Yield by HPLC.

Table 8. The substrate scope of PAN$_{S2}$F-Cu catalyzed A3 coupling reaction conditions.[a)]

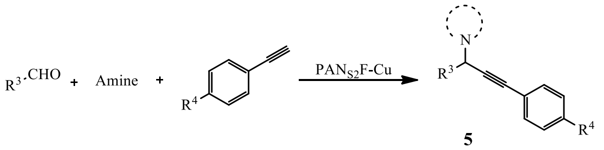

5

Entry	R^3	Amine	R^4	Yield (%)[b)]
1	H	Pyrrolidine	H	5a 96
2	H	Diethylamine	H	5b 92
3	H	Dibutylamine	H	5c 92
4	Isopropyl	Pyrrolidine	H	5d 94
5	Isopropyl	Pyrrolidine	CH_3	5e 93
6	Isobutyl	Pyrrolidine	H	5f 95
7	Ph	Pyrrolidine	H	5g 83
8	Ph	Pyrrolidine	CH_3	5h 84
9	4-$CH_3C_6H_4$	Pyrrolidine	H	5i 80
10	4-$CH_3OC_6H_4$	Pyrrolidine	H	5j 78
11	4-PhC_6H_4	Pyrrolidine	H	5k 75
12	4-BrC_6H_4	Pyrrolidine	H	5l 85
13	4-ClC_6H_4	Pyrrolidine	H	5m 88

[a)] Reaction conditions: aldehyde (1 mmol), amine (1 mmol), alkyne (1.2 mmol), *L*-sodium ascorbate (10 mol%), catalyst (2 mol%, calculate base on Cu) and CH_3CN (5 mL) at 80ºC for 6 h. [b)] Isolate yield.

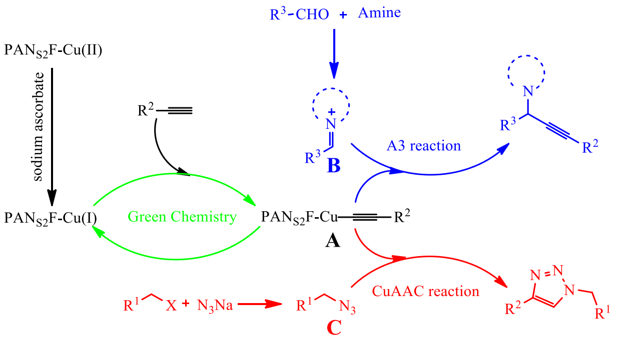

Scheme 2. Possible mechanisms of CuAAC reaction and A3 coupling reaction.

Scaled-up experiment of the CuAAC and A3 reactions catalyzed by PAN$_{S2}$F-Cu

Under the optimal reaction conditions, the CuAAC reaction and A3 reaction catalyzed by PAN$_{S2}$F-Cu were amplified to 50 times. The two one-pot multicomponent reactions were completed without any extension of the reaction time and high product yields of 96% (11.3 g) and 95% (10.8 g), respectively. That shows a potential application in industry of the PAN$_{S2}$F-Cu.

Leaching experiment and recyclability test

The CuAAC reaction of benzyl chloride, phenyl acetylene and sodium azide was chosen as the model reaction to verify the heterogeneity of the PAN$_{S2}$F-Cu. The fiber catalyst was filtrated out at 2 h and then the filtrate continued to stir for next 3 h. As can be seen from Figure 7, the extent of yield was found to remain almost unchanged, indicating no significant leaching of copper ions. Moreover, ICP test confirm that there are no copper ions in the filtrate. These results indicate that the reaction follows a heterogeneous pathway.

One of the highlights of the heterogeneous catalyst is the recyclability which is an important factor from the view of economical and sustainable chemistry.

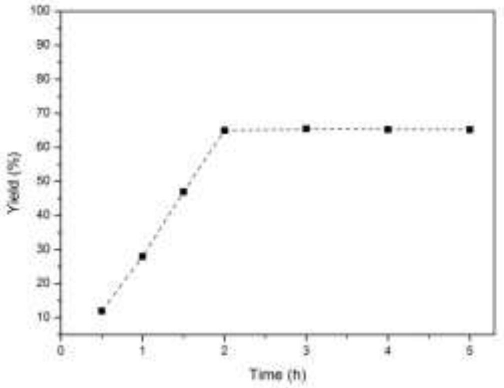

Figure 7. Leaching experiment.

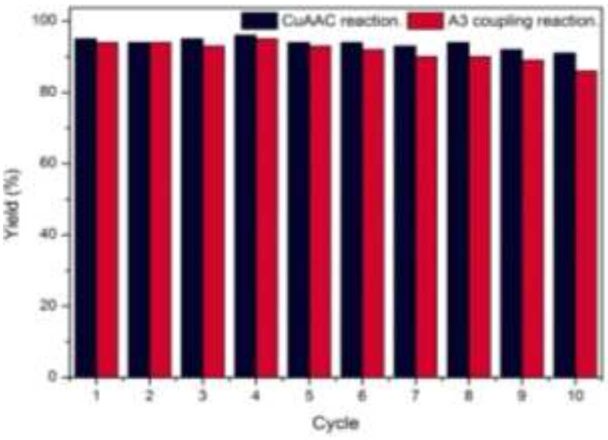

Figure 8. Recyclability of PAN$_{S2}$F-Cu in the CuAAC reaction.

Recyclability of the PAN$_{S2}$F-Cu was investigated using CuAAC reaction with benzyl chloride, phenylacetylene and NaN$_3$ as template and A3 coupling reaction with isobutyraldehyde, pyrrolidine and phenylacetylene as template, and the results are listed in Figure 8. After completion of each reaction, the fiber catalyst was separated out with tweezers and washed with ethyl acetate to remove the adsorbed

Table 9. The compares of different heterogeneous catalytic systems.$^{a)}$

Entry	Catalyst	Condition	Yield (%)/TOF (h^{-1})	Run$^{b)}$
1[49]	Cu/C	H_2O, 100°C, 0.6 h	91/151.7	10
2[25]	CuNPs/C	H_2O, 70°C, 3 h	98/65.3	5
3[50]	Nano-FGT-Cu	H_2O, MW, 120°C, Power 100Watt, 10 min	94/228.3	3
4[51]	HMS-DP-Cu	EtOH, 80°C, 8 h	99/2.5	6
5[52]	P[imCu/IL][Cl]	H_2O/*t*-BuOH, 55°C, 2 h	99/495	12
6$^{c)}$	PAN$_{S2}$F-Cu	H_2O, 60°C, 2 h	97/24.3	10
7[53]	Cu-PS-ala	H_2O, Reflux, 6 h	89/23.7	10
8[19]	Cu@NPs	THF, 60°C, 20 h	95/15.8	5
9[54]	Cu/G	Toluene, 100°C, 4 h	97/8.1	4
10[55]	polymer-supported gold NPs	H_2O, 80°C, 24 h	98/81.7	7
11[56]	SiO_2-Py-CuI	MeCN, 90°C, 6 h	93/3.1	5
12$^{c)}$	PAN$_{S2}$F-Cu	MeCN, 80°C, 6 h	83/6.9	10

$^{a)}$ Take the CuAAC reaction of benzyl bromide and phenylacetylene (entries 1-6) and the A3 coupling reaction of benzaldehyde, pyrrolidine and phenylacetylene (entries 7-12) as template reactions. $^{b)}$ Run: Reused time. $^{c)}$ This work.

product. Then the recycled catalyst was used directly for the next cycle. After used ten times, the reaction can still reach a yield of 93% and 86%, respectively (Figure 8), which indicates that the PAN$_{S2}$F-Cu has an excellent recoverability.

Comparison of the FAN$_{S2}$F-Cu with different heterogeneous catalytic systems

Different heterogeneous catalystic systems are compared with this work and the results are listed in Table 9. The PAN$_{S2}$F-Cu has overwhelming advantages such as low-cost commercial raw material, easy preparation processes, simpl separation of the catalyst with reaction system, high catalytic activity, performing well in scaled-up production and excellent reusability and so on. The PAN$_{S2}$F-Cu has much potential for further applications

Conclusion

Taking advantage of low-cost $Cu(OAc)_2$ as copper source, different Cu(II)-Schiff bases-functionalized polyacrylonitrile fiber catalysts have been prepared and applied to catalyze the CuAAC reaction and A3 coupling reaction. The structures of fiber catalysts have been verified by different characterizations and the structure-activity relationship of the fiber catalyst was investigated. Among the prepared fiber catalysts, the PAN$_{S2}$F-Cu with a hydrophobic micro-environment has shown the best catalytic activities due to the favorable aggregation of reactant on the surface. So it can efficiently promote two reactions with high yields and extensive substrate tolerance. The PAN$_{S2}$F-Cu also performs well in a scaled-up experiment and shows excellent recyclability (at least ten times) in CuAAC reaction and A3 coupling reaction. In addition, the fiber catalyst has very attractive potential for industry application because of the advantages of low cost, easy preparation, excellent flexibility and good mechanical strength.

Experimental Section

General procedure for the CuAAC reaction

A mixture of halohydrocarbon (1 mmol), alkyne (1 mmol), NaN_3 (1.2 mmol), *L*- sodium ascorbate (10 mol%), catalyst (2 mmol%, calculate base on Cu) and water (5 mL) was stirred at 60^{o}C for appropriate time. Then, the fiber catalyst was filtered out and washed with EtOAc (3×10 mL). The filtrate was extracted with ethyl acetate (3×10 m L). The collected organic phases were dried with Na_2SO_4 and the solvent was removed under vacuum to give the corresponding triazole, which did not require any further purification.

General procedure for the A3 reaction

A mixture of aldehyde (1 mmol), amine (1 mmol), alkyne (1.2 mmol), *L*-sodium ascorbate (10 mol%), catalyst (2 mmol%, calculate base on Cu) and CH_3CN (5 mL) was stirred at 80^{o}C for 6 h. Then the fiber catalyst was filtered out and washed with CH_3CN (3×10 mL). The organic phase was collected and the crude product was purified by column chromatography (petroleum ether/ethyl acetate).

Acknowledgements

This was financially supported by the National Natural Science Foundation of China (Nos. 21777111 and 21572156)

References

[1] A. Dömling, I. Ugi, *Angew. Chem.* **2000**, *39*, 3168-3210.

[2] A. Domling, W. Wang, K. Wang, *Chem. Rev.* **2012**, *112*, 3083-3135.

[3] B. Ganem, *Acc. Chem. Res.* **2009**, *42*, 463-472.

[4] M. Barbero, S. Cadamuro, S. Dughera, *Green Chem.* **2017**, *19*, 1529-1535.

[5] Y. M. Yamada, S. M. Sarkar, Y. Uozumi, *J. Am. Chem. Soc.* **2012**, *134*, 9285-9290.

[6] D. Uraguchi, M. Terada, *J. Am. Chem. Soc.* **2004**, *126*, 5356-5357.

[7] S.-i. Ikeda, D.-M. Cui, Y. Sato, *J. Am. Chem. Soc.* **1999**, *121*, 4712-4713.

[8] V. A. Peshkov, O. P. Pereshivko, E. V. Van der Eycken, *Chem. Soc. Rev.* **2012**, *41*, 3790-3807.

[9] V. V. Rostovtsev, L. G. Green, V. V. Fokin, K. B. Sharpless, *Angew. Chem. Int. Ed.* **2002**, *41*, 2596-2599.

[10] J. Lauko, P. H. J. Kouwer, A. E. Rowan, *J. Heterocycl. Chem.* **2017**, *54*, 1677-1699.

[11] M. S. Costa, N. Boechat, E. A. Rangel, C. da Silva Fde, A. M. de Souza, C. R. Rodrigues, H. C. Castro, I. N. Junior, M. C. Lourenco, S. M. Wardell, V. F. Ferreira, *Bioorg. Med. Chem.* **2006**, *14*, 8644-8653.

[12] Y. H. Lau, P. J. Rutledge, M. Watkinson, M. H. Todd, *Chem. Soc. Rev.* **2011**, *40*, 2848-2866.

[13] L. Liang, D. Astruc, *Coord. Chem. Rev.* **2011**, *255*, 2933-2945.

[14] F. T. Zindo, J. Joubert, S. F. Malan, *Future Med. Chem.* **2015**, 7, 609-629

[15] C. J. Li, *Acc. Chem. Res.* **2010**, 43, 581-590

[16] P. T. Anastas, M. M. Kirchhoff, *Acc. Chem. Res.* **2002,** *35*, 686-694.

[17] A. Pourjavadi, Z. Habibi, *RSC Adv.* **2015**, *5*, 99498-99501.

[18] M. Lee, B.-Y. Chen, W. Den, *Appl. Sci.* **2015**, *5* (4), 1272-1283.

[19] M. Gholinejad, F. Saadati, S. Shaybanizadeh, B. Pullithadathil, *RSC Adv.* **2016**, *6*, 4983-4991.

[20] E. Ozkal, S. Özçubukçu, C. Jimeno, M. A. Pericàs, *Catal. Sci. Technol.* **2012**, *2*, 195-200.

[21] a) Y. Yang, J. Guan, P. Qiu, Q. Kan, *Appl. Surf. Sci.* **2010**, *256*, 3346-3351; b) Y. Yang, Y. Zhang, S. Hao, J. Guan, H. Ding, F. Shang, P. Qiu, Q. Kan, *Appl. Cat., A* **2010**, *381*, 274-281.

[22] M. Nasr-Esfahani, I. Mohammadpoor-Baltork, A. R. Khosropour, M. Moghadam, V. Mirkhani, S. Tangestaninejad, H. Amiri Rudbari, *J. Org. Chem.* **2014**, *79*, 1437-1443.

[23] F. Nador, M. A. Volpe, F. Alonso, A. Feldhoff, A. Kirschning, G. Radivoy, *Appl. Cat., A* **2013**, *455*, 39-45.

[24] S. Kumari, A. Shekhar, D. D. Pathak, *RSC Adv.* **2016**, *6*, 15340-15344.

[25] F. Alonso, Y. Moglie, G. Radivoy, M. Yus, *Adv. Synth. Catal.* **2010**, *352*, 3208-3214.

[26] C. A. McNamara, M. J. Dixon, M. Bradley, *Chem. Rev.* **2002**, *102*, 3275-3300.

[27] L. Zhang, Z. Li, R. Chang, Y. Chen, W. Zhang, *React. Funct. Polym.* **2009**, *69*, 234-239.

[28] H. B. Sadeghi, H. A. Panahi, M. Abdouss, B. Esmaiilpour, M. N. Nezhati, E. Moniri, Z. Azizi, *J. Appl. Polym. Sci.* **2013**, *128*, 1125-1130.

[29] M.-L. Wang, T.-T. Jiang, Y. Lu, H.-J. Liu, Y. Chen, *J.Mater. Chem. A* **2013**, *1*, 5923.

[30] S. Mu, J. Guo, Y. Yu, Q. An, S. Zhang, D. Wang, S. Chen, X. Huang, S. Li, *Energy Convers. Manage.* **2016**, *110*, 176-183.

[31] X. Shen, Y. Ji, J. Wang, *J. Appl. Polym. Sci.* **2008**, *110*, 313-320.

[32] S. Jain, S. Chattopadhyay, R. Jackeray, H. Singh, *Anal. Chim. Acta.* **2009**, *654*, 103-110.

[33] A. G. Gonçalves, J. Moreira, J. P. S. Sousa, J. L. Figueiredo, M. F. R. Pereira, J. J. M. Órfão, *Catal. Today* **2015**, *249*, 59-62.

[34] a) G. Li, L. Zhang, Z. Li, W. Zhang, *J Hazard Mater* **2010**, *177*, 983-989; b) J. Cao, G. Xu, Y. Xie, M. Tao, W. Zhang, *RSC Adv.* **2016**, *6*, 58088-58098.

[35] a) P. Li, J. Du, Y. Xie, M. Tao, W.-Q. Zhang, *ACS Sustainable Chem. Eng.* **2016**, *4*, 1139-1147; b) X.-L. Shi, M. Tao, H. Lin, W. Zhang, *RSC Adv.* **2014**, *4*, 64347-64353.

[36] X.-L. Shi, X. Xing, H. Lin, W. Zhang, *Adv. Synth. Catal.* **2014**, *356*, 2349-2354.

[37] J. Du, G. Xu, H. Lin, G. Wang, M. Tao, W. Zhang, *Green Chem.* **2016**, *18*, 2726-2735.

[38] J. Du, M. Tao, W. Zhang, *ACS Sustainable Chem. Eng.* **2016**, *4*, 4296-4304.

[39] J. Cao, G. Xu, P. Li, M. Tao, W. Zhang, *ACS Sustainable Chem. Eng.* **2017**, *5*, 3438-3447.

[40] J. Du, B. Shuai, M. Tao, G. Wang, W. Zhang, *Green Chem.* **2016**, *18*, 2625-2631.

[41] a) J. S. Johnson, D. A. Evans, *Acc. Chem. Res.* **2000**, *33* (6), 325-335; b) R. Prasad, P. Singh, *Catal. Rev.* **2012**, *54*, 224-279.

[42] R. Antony, S. T. David Manickam, P. Kollu, P. V. Chandrasekar, K. Karuppasamy, S. Balakumar, *RSC Adv.* **2014**, *4*, 24820.

[43] M. Kazemnejadi, A. R. Sardarian, *RSC Adv.* **2016**, *6*, 91999-92006.

[44] A. Kaur, S. Mann, B. Goyal, B. Pal, D. Goyal, *RSC Adv.* **2016**, *6*, 102733-102743.

[45] S.-P. Rwei, T.-F. Way, W.-Y. Chiang, S.-Y. Pan, *Colloid and Polym. Sci.* **2017**, *295*, 803-815.

[46] P. Li, Y. Liu, J. Cao, M. Tao, W. Zhang, *ChemCatChem* **2017**, *9*, 3725-3732.

[47] F. Himo, T. Lovell, R. Hilgraf, V. V. Rostovtsev, L. Noodleman, K. B. Sharpless, V. V. Fokin, *J. Am. Chem. Soc.* **2005**, *127*, 210-216.

[48] L. Lili, Z. Xin, G. Jinsen, X. Chunming, *Green Chem.* **2012**, *14*, 1710.

[49] H. Sharghi, R. Khalifeh, M. M. Doroodmand, *Adv. Synth. Catal.* **2009**, *351*, 207-218.

[50] R. B. Nasir Baig, R. S. Varma, *Green Chem.* **2012**, *14*, 625-632.

[51] B. Lai, Z. Huang, Z. Jia; R. Bai, Y. Gu, *Catal. Sci. Technol.* **2016**, *6*, 1810-1820.

[52] A. Pourjavadi, S. H. Hosseini, F. Matloubi Moghaddam, S. E. Ayati, *RSC Adv.* **2015**, *5*, 29609-29617.

[53] M. M. Islam, A. S. Roy, S. M. Islam, *Catal. Lett.* **2016**, *146*, 1128-1138.

[54] S. Frindy, A. El Kadib, M. Lahcini, A. Primo, H. García, *Catal. Sci. Technol.* **2016**, *6*, 4306-4317.

[55] C. Nájera, M. Gholinejad, F. Hamed, *Synlett* **2016**, *27*,1193-1201.

[56] P. Likhar, S. Roy, M. Roy, M. Subhas, M. Kantam, R. De, *Synlett* **2007**, *2007*, 2301-2303.

FULL PAPER

Copper(II)-Schiff Base Complex-Functionalized Polyacrylonitrile Fiber as a Green Efficient Heterogeneous Catalyst for One-Pot Multicomponent Syntheses of 1,2,3-Triazoles and Propargylamines

Adv. Synth. Catal. **Year**, *Volume*, Page – Page

Pengyu Li,[a] Yuanyuan Liu,[a] Lu Wang,[a] Jian Xiao,[a] Minli Tao[a]*